Histologic and Histomorphometric Behavior of Microgrooved Zirconia Dental Implants with Immediate Loading

Rafael Arcesio Delgado-Ruiz, DDs, MsC, PhD;* Jose Luis Calvo-Guirado, DDs, MsC, PhD;†
Marcus Abboud, MD, MsC, PhD;‡ Maria Piedad Ramirez-Fernandez, DDs, MsC, PhD;§
Jose Eduardo Mate-Sanchez, DDs, MsC, PhD;¶ Bruno Negri, DDs, MsC, PhD;**
Daniel Rothamel, MD, MsC, PhD††

ABSTRACT

Purpose: The study aims to assess the total soft tissue (ST) width, crestal bone level (CBL), bone-to-implant contact (BIC), and bone density (BD) for zirconia implants textured with microgrooved surfaces and immediately loaded.

Materials and Methods: This study included 51 implants; one implant from each study group was retained for surface characterization. The 48 remaining implants were inserted randomly in premolar areas of both sides of the healed edentulous lower jaws of foxhound dogs. They were divided into three groups of 16: control (titanium); test A (zirconia), and test B (microgrooved zirconia). The implants were splinted and covered with an acrylic bridge. A split-mouth design was used and immediate occlusal loading was applied on one side, while the other side did not have occlusal contact. ST, CBL, BIC, and BD were evaluated after 3 months. The effects of immediate loading on these parameters were analyzed.

Results: All the implants were osseointegrated. ST was established at 3 months with mean values of 2.9 ± 0.4 mm for all groups. No differences were appreciated between loaded and unloaded sides regarding ST ($p > .05$). CBL showed a mean of 1.2 ± 0.3 mm for all groups without differences between loaded and unloaded sides ($p > .05$). BIC percentages were significantly higher for loaded all-microgrooved implants ($p < .05$). BD percentages were higher in areas close to all-microgrooved implants ($p < .05$) and significantly higher for loaded implants than unloaded.

Conclusions: Within the limitations of the present study, it may be concluded that for zirconia dental implants with microgrooved surfaces and immediate loading, the thickness of STs remains stable resulting in 3 mm mean biologic width, that crestal bone preservation is related to insertion depth, and that higher BIC percentages and increased BD around implants microgrooved over the entire intraosseous area may be expected at 3 months following implant insertion and immediate loading.

KEY WORDS: BIC, bone density, crestal bone preservation, dental implants, histomorphometry, immediate loading, zirconia

INTRODUCTION

In spite of the proven long-term reliability of titanium implants,[1–4] some disadvantages have been reported which appear in either the short term or the long term,

*Assistant professor, Department of Prosthodontics and Digital Technology, School of Dental Medicine, Stony Brook University, Stony Brook, NY, USA; †associate professor, chairman of Implant Dentistry, Faculty of Medicine and Dentistry, Murcia University, Murcia, Spain; ‡associate professor and chairman, Department of Prosthodontics and Digital Technology, School of Dental Medicine, Stony Brook University, Stony Brook, NY, USA; §assistant professor, Department of Implant Dentistry, Faculty of Medicine and Dentistry, Murcia University, Murcia, Spain; ¶associate professor, Department of Implant Dentistry, Faculty of Medicine and Dentistry, Murcia University, Murcia, Spain; **assistant professor, Faculty of Medicine and Dentistry, Murcia University, Murcia, Spain; ††assistant professor, Department of Oral and Maxillofacial Plastic Surgery, University of Cologne, Cologne, Germany

Reprint requests: Prof. Rafael Arcesio Delgado-Ruiz, Department of Prosthodontics and Digital Technology, School of Dental Medicine, Stony Brook University, 1104 Westchester Hall, Stony Brook, NY 11794-7812, USA; e-mail: raderu78@gmail.com; rafael.delgado-ruiz@stonybrookmedicine.edu

DOI 10.1111/cid.12069

including allergies or sensitivity to the titanium,[5–8] the occurrence of gingival shrinkage and gingival translucency, which can leave the dark/gray color of the titanium exposed to view in the esthetic zone of the upper maxilla in cases of thin gingival biotypes,[9–14] and lastly, the electrical conductivity and corrosive properties of titanium, which can affect osseointegration in some cases.[15,16]

These factors have led researchers to explore other materials as possible alternatives to titanium for fabricating dental implants.

Partially stabilized tetragonal zirconium dioxide ceramic materials with yttrium, manufactured under high pressure and at high temperatures, produce a noticeable increase in mechanical properties of resistance to compression forces and to fracture.[17–19] They also possess positive optical qualities of light transmission, an attractive characteristic when it comes to the fabrication of dental implants for placement in the esthetic zone,[20] as well as other positive properties, such as excellent biocompatibility both in vitro[21,22] and in vivo,[23,24] low bacterial and pathogen adherence,[25,26] and a capacity for osseointegration similar to titanium.[27,28]

In order to improve the osseointegration of zirconia implants, various surface modifications have been applied to experimental implants, including the creation of tunnel-shaped round perforations in zirconia laminar implants,[29] airborne-particle abraded implant surfaces with different granulometries,[30] surfaces treated with pore-forming substances,[31] surfaces machined or sandblasted with Al_2O_3 particles of 250 μm diameter,[32] sandblasting combined with acid etching,[33] application of pore-forming substances to create surface pores of different sizes,[34] nanometric modifications,[35,36] surface covering with layers of calcium-liberating titanium oxide,[27] coverings of bioactive ceramic,[24] or sandblasting with the addition of nano-retainers.[37]

Such modifications can improve initial healing, resistance to removal torque, and bone-to-implant contact (BIC) with positive effects on the maintenance of osseointegration.

The hypothesis that any modification of zirconia implant surface will result in implant damage was studied by Silva and colleagues[38] who showed that an applied force of 600 N on the abutment of one-piece ceramic implants did not influence the expected life time after 50,000 cycles and concluded that the failure depended upon the magnitude of the applied load at the level of the second thread's internal diameter, even mechanical tests have been made in partially hollow and porous zirconia implants and based on an evaluation of bending strength, hardness, fracture toughness, and fatigue life of implant substrates, showed structural properties comparable with the requirements for implants[39,40]

Laser treatment for zirconia implants would be a response to reduce mechanical damage induced by surface treatments.

Recently, our research team made a modification to a zirconia implant using femtosecond laser to create microgrooves and micropores of 30 μm in diameter on a 2 mm stretch of the implant collar in the intraosseous portion. This resulted in a reduction in Al and C surface contaminants, an increase in oxygen presence, increased surface roughness, no affectation of the tetragonal crystalline phase, and a clean and homogenous surface.[41]

As no research into the osseointegration of zirconia implants microgrooved in the intraosseous portion has been published to date, the present study is a further step in our ongoing research into the clinical application of the surface modification described previously.

The objective of this study, therefore, was to test in vivo, using histologic and morphometric analysis, the effects of the addition of microgrooves to the intraosseous portion of zirconia implants, quantifying total soft tissue (ST), crestal bone loss (CBL), BIC, and peripheral bone density (BD) and the effects on these parameters resulting from immediate loading versus no loading at 3 months.

MATERIALS AND METHODS

Six foxhound dogs of approximately 1 year of age, each weighing between 14 and 15 kg were used in the experiment. The Ethics Committee for Animal Research at the University of Murcia, Spain, approved the study protocol which followed guidelines established by the European Union Council Directive of November 24, 1986 (86/609/EEC). The animals were fed a daily pellet diet. Clinical examination determined that the dogs were in good general health, with no systemic involvement.

Surgical Procedure

The animals were pre-anesthetized with acepromazine 0.2–1.5 mg/kg 10 minutes before being administered butorphanol (0.2 mg/kg) and medetomidine (7 mg/kg). The mixture was injected intramuscularly in the femoral

quadriceps. An intravenous catheter was inserted in the cephalic vein and propofol was infused at a slow, constant rate of 0.4 mg/kg/min. Local infiltrative anesthesia was administered at the surgical sites. These procedures were carried out under the supervision of a veterinary surgeon. Bilateral mandibular tooth extractions (P2, P3, P4, and M1) were performed. An intrasulcular incision was performed from mesial of P2 to mesial of M2 and a marginal flap of 2 mm was released. The teeth were sectioned in a buccolingual direction at the bifurcation using a tungsten carbide bur; the roots were extracted individually using a periotome and forceps, without damaging the bony walls. Wound closure was carried out using single resorbable sutures (Dexon 3-0, Davis & Geck, American Cyanamid Co., Wayne, NJ, USA).

During the first week after surgery, the animals received antibiotics and analgesics: amoxicillin (500 mg twice daily) and ibuprofen (600 mg three times a day) via the systemic route. The dogs were fed a soft diet for 14 days and a pellet diet thereafter

Implants

Surface Characterization. A Veeko NT 1100® non-contact interferometric microscope (Wyco Systems, New York, NY, USA) was used to quantify surface roughness parameters. One implant per group was analyzed, a magnification of ×20.7 was used in vertical scanning interferometry mode within the intraosseous portion of the implant surfaces at the tops, flanks, and valleys (10 measurements per implant selected randomly at transversal and vertical directions were performed at each zone) and the arithmetic mean of the absolute values of the surface height within the sampling area (S_a), average space between irregularities crossing the mean plane (S_{cx}), and developed surface area ratio (S_{dr}) parameters were determined.

To separate roughness from waviness and shape for digital three-dimensional measurements, on a micrometer scale, a highpass gaussian filter of 100×100 μm was used on measured areas of 290×290 μm.

After this, the implants were degreased in ethanol solutions and desiccated with acetone. A JEOL-6100 scanning electron microscope (Jeol Ltd. Tokyo, Japan) was used to study surface topography. Element analysis was carried out by Energy Dispersive x-ray spectroscopy, using an OXFORD INCA 300 system (Oxford Instruments, Abingdon, Oxfordshire, United Kingdom). All the specimens were coated with a thin layer of conductive carbon in a sputter-coating unit (SCD 004 Sputter-Coater with OCD 30 attachment, Bal-Tec, Vaduz, Liechtenstein, Germany). Elemental analysis was carried out in ten sampling areas with the same dimensions in the intraosseous portion of the implant surfaces. The observation parameters used were a focal distance of 32 mm, 20 Kv, and ×100 magnification.

Implant Insertion Procedure

Implants were placed after a 2-month healing period. After crestal incision, a full thickness flap was reflected and each site was prepared following the protocol recommended by the implant manufacturer (Bredent Medical® GMBH & Co. KG, Senden, Germany), preparing a bed of 4 mm diameter and 10 mm length, each separated from the neighboring perforation by 3–3.5 mm. Each hemimandible received four tapered screw implants, inserted with torque values ≥35 Ncm, all with the same dimensions and geometry at the intraosseous portion. The implant type and position were randomly assigned using special software (Research Randomizer 3.0, from www.randomizer.org).

Forty-eight implants of 4 mm diameter and 10 mm length were placed, divided into three groups: *Control*: 16 titanium Blue-sky® implants, made from titanium grade IV with a surface sandblasted with alumina oxide particles of 350 μm-550 μm and acid etched with a bath of sulfuric acid at 37% 1 hour (Bredent Medical GMBH & Co. KG); *Test A*: 16 White SKY implants made from zirconia, with a surface sandblasted with alumina oxide particles of 350–550 μm (Bredent Medical GMBH & Co. KG); *Test B*: 16 White SKY zirconia implants made from zirconia, with a surface sandblasted with alumina oxide particles of 350–550 μm (Bredent Medical GMBH & Co. KG) treated with femtosecond laser pulses to create 30 μm wide, 70 μm pitch length microgrooves over the entire intraosseous surface with a method previously described.[41]

Briefly, a commercial Ti:Sapphire oscillator (Tsunami, Spectra-Physics, Stahnsdorf, Germany) and a regenerative amplifier system (Spitfire, Spectra-Physics) based on chirped pulsed amplification were used for microstructuring. The system delivers 120 fs linearly polarized pulses at 795 nm with a repetition rate of 1 kHz. The transverse mode was TEM00, and the beam width was 9 mm, maximum beam energy of 1.1 mJ (Figure 1).

The zirconia implant body has a one-piece design that includes the abutment and so, in order to create similar conditions for the Control Group implants, the

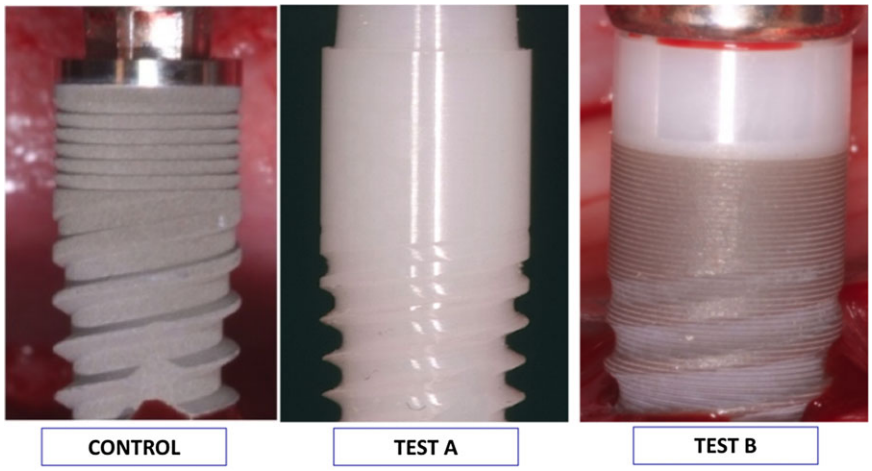

Figure 1 Images of different implant types studied. The implants have the same geometry but the following differences: *A*, Titanium control implant has microspirals in collar area; *B*, Zirconia test A implant with sandblasted surface; *C*, Zirconia test B implant with sandblasted surface microgrooves over the entire intraosseous surface.

titanium implants received machined abutments SKY-EM00® (Bredent Medical GMBH & Co. KG), which were screwed to the implants at 25 Ncm. All implant abutments received a specially fabricated polyether ether ketone (PEEK) cap and were then splinted using 0.16 mm orthodontic ligature and reinforced acrylic resin Pi-Ku-Plast HP 36 (Bredent Medical GMBH & Co. KG). A split-mouth design was applied: one side was subjected to immediate occlusal loading, verifying the presence of occlusal contact points using articulating paper of 100 µm width (Bausch Progress 100®, Dr. Jean Bausch KG, Köln, Germany) by manually induced opening and closing movements; on the other side, the contact points were located, reduced, and eliminated by the same method, establishing a minimum space of 2 mm between the acrylic splint and the opposing teeth.

During the first week following surgery, the animals received antibiotics and analgesics amoxicillin (500 mg twice daily) and ibuprofen (600 mg three times a day) via the systemic route. The sutures were removed after 2 weeks. The dogs were fed a soft diet during the entire experimental period to protect the temporal acrylic splints from fractures. Healing was evaluated weekly and plaque control was maintained by flushing the oral cavity with chlorhexidine digluconate.

Histologic and Histomorphometric Procedures

Three months following implant placement, the animals were euthanized by means of an overdose of pentotal Natrium® (Abbot Laboratories, Madrid, Spain) and mandibular block resections were retrieved for analysis. The samples were fixed in formaldehyde and dehydrated in a graded series of ethanol up to 100%. The implants and surrounding bone were embedded in methylmethacrylate (Technovit 7100®, Heraeus Kulzer, Wehrheim, Germany). Thick sections measuring 100 µm along the axis of each implant were cut in vestibular-lingual direction using a diamond saw microsectioning system (Exakt-Apparatebau, Norderstedt, Germany). These sections were reduced to 80 µm thickness using grinding techniques. Three middle sections were obtained per implant. A toluidine blue stain was applied. The sections were imaged and analyzed using light microscopy (Olympus BX 61, Hamburg, Germany).

Histomorphometry

Histomorphometric analysis evaluated soft and hard tissues. Total ST evaluation was calculated by measuring in millimeters the distance between the most coronal aspect of the STs and the most coronal BIC. CBL was evaluated by measuring the distance from implant shoulder in the case of zirconia implants, or from the platform in the case of titanium implants, to the first point of BIC in millimeters.

BIC for each histologic section was calculated by quantifying the length of implant surface in contact with bone tissue, compared with the total implant surface length, expressed as a percentage.

BD measurements evaluated the percentages of mineralized bone in relation to the percentages of marrow spaces, measured and compared in two

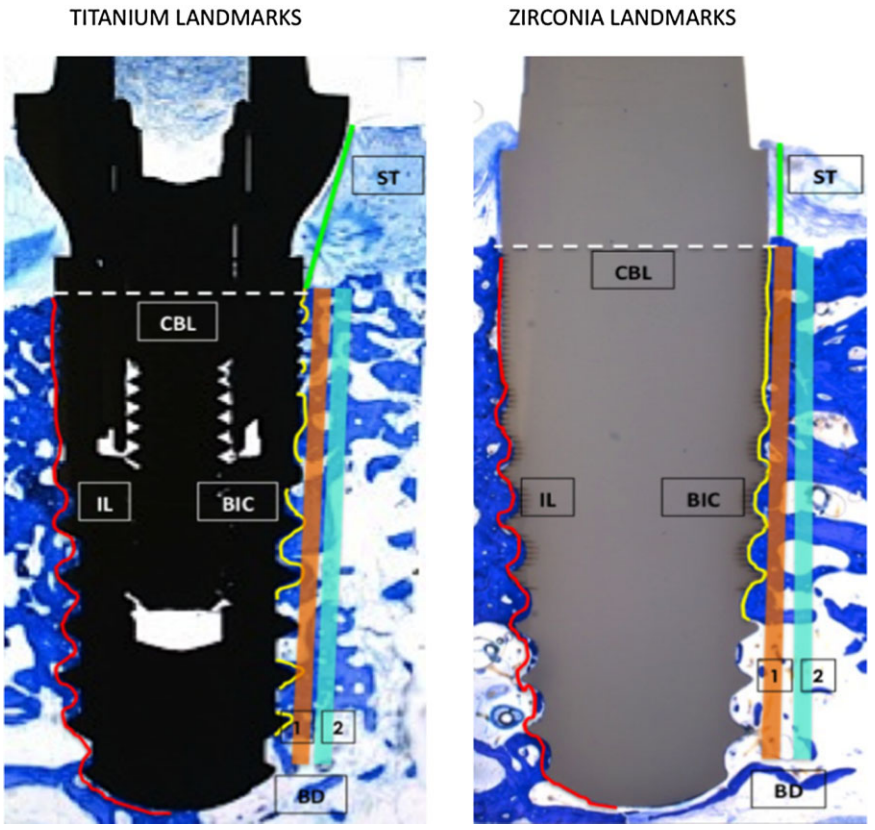

Figure 2 Landmarks for histomorphometry. Titanium implant appears as black color. Zirconia implant appears in gray. White dotted horizontal line marks implant insertion level, red line shows total IL, yellow line shows areas of BIC. Orange bar shows BD close to implant (BD_1), green bar shows peripheral BD (BD_2). ST, soft tissue; CBL, crestal bone loss; IL, implant length; BIC, bone-to-implant contact; BD, bone density.

rectangular regions of 8 mm length × 1 mm width parallel to the axis of the implant body, the first adjacent to the implant (BD_1) and the other of equal dimensions in peripheral bone taken as a reference (BD_2). The BD_1 area was defined by placing a borderline at the tips of the threads, parallel to the implant's longitudinal axis. The BD_2 area was selected from an area parallel to and with the same dimensions as BD_1, at 500–1,000 µm distance, within the host bone.

Histomorphometry was performed using a video camera (Sony 3CCD, Berlin, Germany) at ×12.5 and ×40 magnification. The images were digitalized (Axiophoto System, Carl Zeiss, Jena, Germany) and landmarks were fixed and measured (Figure 2).

Statistical Analysis

Descriptive statistics were used to analyze the histomorphometric data of ST, CBL, BIC BD_1, and BD_2 (mean values and standard deviations); the mesial and distal aspects of each implant section were averaged to a mean value per section.

For statistical evaluation of the changes within groups, the paired *t*-test was applied; for comparisons between groups, the unpaired *t*-test was used. The error was set at 0.05.

The dog was used as a unit for analysis ($n = 6$), using average results across similarly treated implants in the same dog, which were then compared.

RESULTS

Surface Characterization

Test B implants had the greatest surface roughness expressed as S_a, this being threefold greater than test A implants, and twofold more roughness than the control group. The titanium implants showed slightly greater surface roughness than test A (Figure 3 and Table 1).

The surface composition of zirconia implants in test A showed mainly ZrO_2 as well as carbon and aluminum; carbon and aluminum were observed in smaller amounts in test B. Control implant surfaces were mainly composed of titanium with minimal detection of

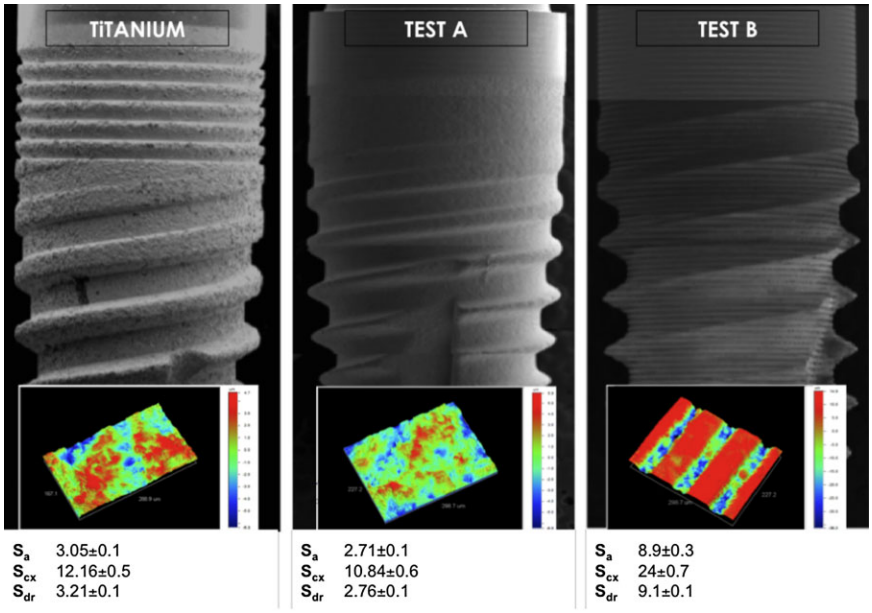

Figure 3 SEM and profilometry images of implants. Left hand image shows a control titanium implant with sandblasted plus acid-etched surface, central image shows a test A zirconia implant with a sandblasted surface, right hand image shows a test B zirconia implant sandblasted plus microgrooved. The colored images displayed at the base are typical profilometry measurements with the mean roughness values obtained. Red color indicates highest roughness values, while blue color indicates lower roughness values. SEM magnification ×15.

carbon and aluminum, oxygen was present as TiO_2. No additional elements were detected (Table 2).

Clinical Data

Wear to the acrylic splints was observed clinically with some areas of exposure of the PEEK caps. No acrylic splint fractures were observed. No implants fractured on acrylic splint removal, and a better ST appearance was appreciated for all zirconia implants compared with titanium. All implants were osseointegrated during the experimental time.

TABLE 1 Surface Roughness Parameters S_a, S_{cx}, S_{dr} (Mean Averages ± Standard Deviation)

Surface Roughness	S_a (μm)	S_{cx} (μm)	S_{dr} (μm)
Control			
Top	3.32 ± 0.2	13.52 ± 0.6	3.52 ± 0.2
Valley	3.05 ± 0.1	12.16 ± 0.5	3.21 ± 0.1
Flank	3.12 ± 0.1	12.93 ± 0.6	3.36 ± 0.1
Test A			
Top	2.83 ± 0.2	11.53 ± 0.5	2.94 ± 0.1
Valley	2.71 ± 0.1	10.84 ± 0.6	2.76 ± 0.1
Flank	2.75 ± 0.1	11.12 ± 0.4	2.85 ± 0.1
Test B			
Top	9.6 ± 0.62	26. ± 0.9	10.02 ± 0.1
Valley	8.9 ± 0.3	24 ± 0.7	9.1 ± 0.1
Flank	9.2 ± 0.5	25 ± 0.8	9.5 ± 0.1

S_a, arithmetic mean of the departures of the roughness area from the mean plane; S_{cx}, average spacing between the irregularities crossing the mean plane; S_{dr}, developed surface area ratio, that is, a ratio between the three-dimensional measurement and a two-dimensional reference plane. The S_a, S_{cx}, and S_{dr} values were higher for test B, while test A showed the lower values of surface roughness.

Histologic and Histomorphometric Analysis

Histologic observations showed that STs for all implants in all groups were covered by a keratinized oral epithelium that continued from the peri-implant marginal mucosa and was continuous with the barrier epithelium facing the implants. The peri-implant bone surrounding immediately loaded implants (Figure 4) showed a more dense aspect compared with the peri-implant bone surrounding unloaded implants (Figure 5).

The total mean width of ST was very similar between groups, with no significant differences between loaded and unloaded implants ($p > .05$) (Figure 6 and Table 3).

CBL was an average of 1.2 ± 0.05 mm in test B and the control group, which were slightly lower than test A, but without significant differences between groups. Loading did not result in any effect on CBLs ($p > .05$) (Table 4).

Lamellar bone architecture was characterized by a high density of osteons around all the implant surfaces.

TABLE 2 Elements Present in Surface Expressed as Percentages

EDX Surface Analysis	C%	Al%	O%	Zr%	Ti%
Titanium control ($n = 1$)	2.3 ± 1.7	1.7 ± 0.3	15 ± 0.6	0	81 ± 1.3
Zirconia test A ($n = 1$)	19.7 ± 0.8	4.3 ± 0.9	12.6 ± 0.5	60.2 ± 0.7	0
Zirconia test B ($n = 1$)	0.3 ± 0.12*	0.18 ± 0.1*	23.1 ± 0.12*	76.3 ± 0.2*	0

Mean ± standard deviation. In zirconia implants treated with microgrooves, percentages of carbon and aluminum were reduced while oxygen and zirconium increased significantly. Titanium implants presented less carbon and aluminum.
*$p < .005$.

All implants showed signs of natural bone remodeling. In some areas, there was darker stained new bone in direct contact with the implant surface and adjacent areas of mature osteons and marrow spaces that demonstrated remodeling activity. Blood vessels were observed in direct contact with implant surfaces in all groups (Figure 7a–c).

BIC was higher with immediately loaded implants in all groups compared with unloaded implants ($p < .05$). Test B group showed higher values than the other groups for both unloaded (test B 48 ± 7%, control 43 ± 6%, test A 36 ± 6%) and immediately loaded implants (test B 78 ± 5%, control 57 ± 6%, test A 48 ± 3%; $p < .05$; Figure 8).

A close-up view of some threads showed direct contact with the surrounding bone, with mature and new bone in all cases; test B implants showed an additional bone growth toward and inside the microgrooved area (Figures 9–11).

A close-up view of some inter-thread areas shows complete bone filling in control implants (Figure 12); for test A implants in some areas, the front of bone growth moves from the surrounding bone to the implant surface, covered with a layer of non-mineralized matrix (Figure 13). Test B implants showed additional bone growth and Haversian systems in contact with the microgrooves, as well as a more apparent remodeling process represented by numerous areas cement lines and mature and new bone (Figure 14). The lowest BIC values were observed in test A implants with either immediately loaded or unloaded conditions.

Within individual animals, in *t*-test comparisons, BD_1 values were higher for Test B, followed by the control group and test A, while BD_2 values were lower compared with BD_1 ($p < .05$). In relation to loading, the BD_1 and BD_2 were higher for immediately loaded implants throughout the sample ($p < .05$) (Table 5).

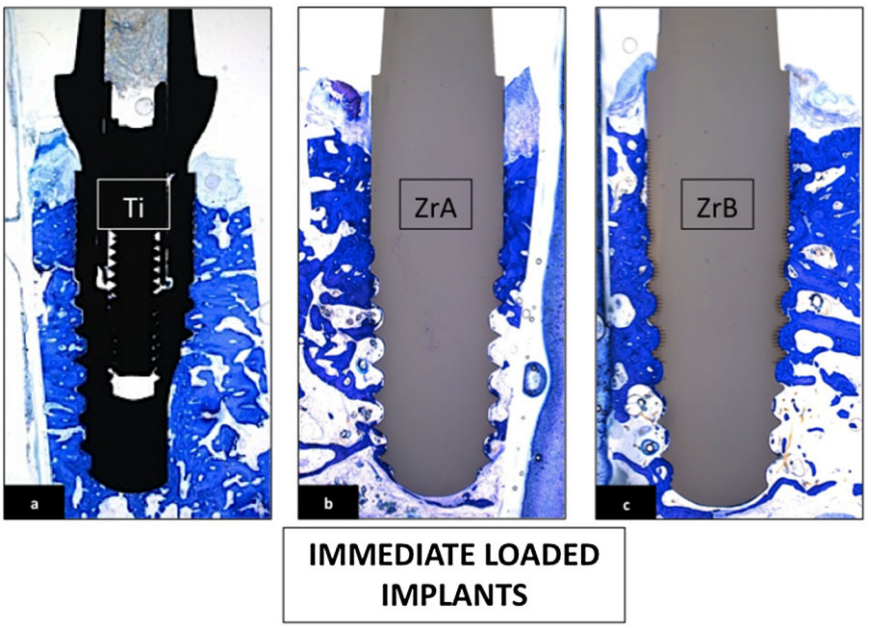

Figure 4 Histologic panoramic view of immediately loaded implants. Samples include implant, soft tissue, and hard tissue. *A*, Control implant. *B*, Test A zirconia implant. *C*, Test B zirconia implant. Toluidine blue stain; ×12.5 magnification.

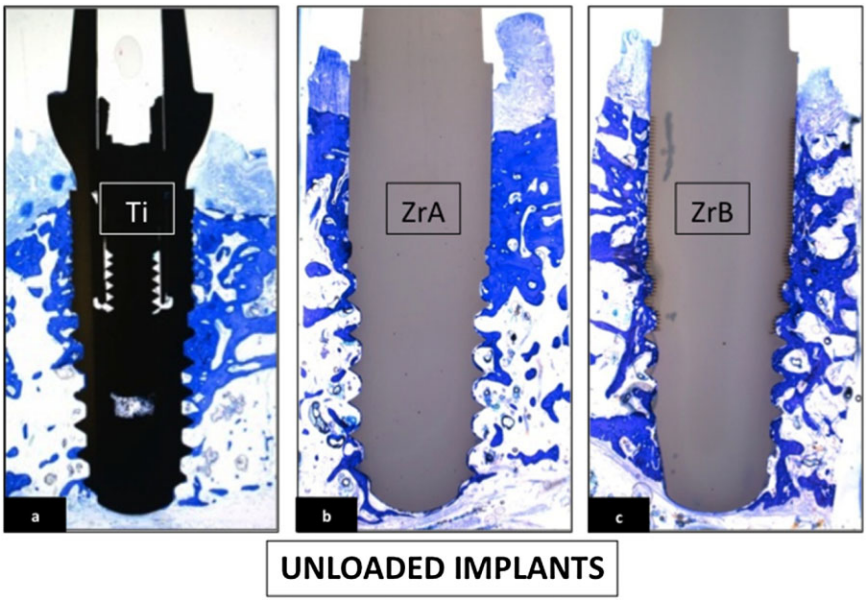

Figure 5 Histologic panoramic view of unloaded implants. Samples included implant, soft tissue, and hard tissue. *A*, Control implant. *B*, Test A zirconia implant. *C*, Test B zirconia implant. All groups showed lower bone formation compared with the immediately loaded implants. Toluidine blue stain; ×12.5 magnification.

DISCUSSION

The aim of this study was to test the biologic effects of the addition of microgrooves to the intraosseous surfaces of zirconia implants after three months and to determine if this surface modification positively or negatively affects ST thickness, crestal bone height, BIC, and BD under immediately loaded and unloaded conditions.

Titanium implants with sandblasted, acid-etched surfaces were used as the control group as their behavior has already been extensively researched.[42,43]

Chemical surface composition in all the groups showed some carbon content probably because the carbon coating layer was present. The aluminum was present in all groups probably due some sandblasting remnants, lower amounts of aluminum were detected in controls that received a posterior acid etching and test B that received a posterior laser treatment that could reduce the aluminum content; however, test A that only receives the sandblasting process without any additional treatment showed more aluminum content.

The selected slice thickness of 80 µm was chosen due to technical complications that occur with lower thicknesses of resin-embedded zirconia bone samples, which when subjected to ground and polishing results in

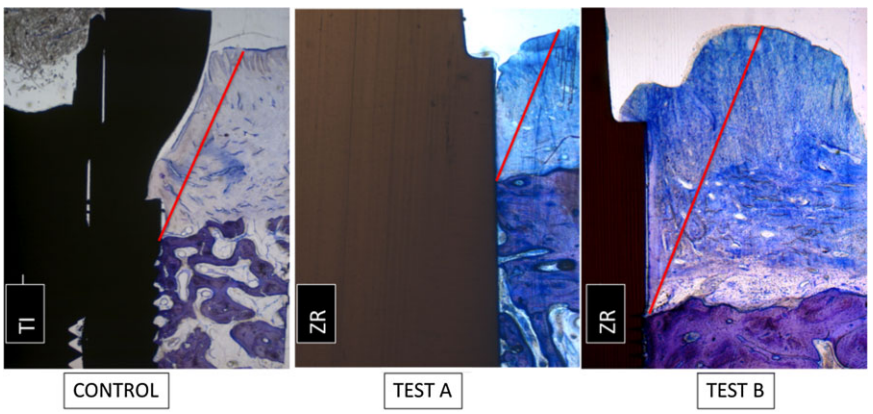

Figure 6 Total soft tissue. The red line shows the borders from bone-to-implant contact to the most coronal aspect of the gingiva. Soft tissue growth covers part of the abutment area in all groups. Toluidine blue stain; ×12.5 magnification.

TABLE 3 Total Soft Tissue Expressed as Millimeters for Immediately Loaded and Unloaded Implants

	ST (Total Soft Tissue), mm	
	Immediately Loaded	Unloaded
Titanium control, $n = 16$	3.12 ± 0.12	3.07 ± 0.3
Zirconia test A, $n = 16$	2.78 ± 0.18	2.80 ± 0.17
Zirconia test B, $n = 16$	2.82 ± 0.23	2.83 ± 0.21
p^*	NS	NS
	0.894	0.786

Mean ± standard deviation, *t*-test. No significant differences were found between immediately loaded and unloaded implants.
*$p > .05$.

TABLE 4 Crestal Bone Loss (CBL) Expressed as Millimeters, for Immediately Loaded and Unloaded Implants

	CBL, mm	
	Immediately Loaded	Unloaded
Titanium control, $n = 16$	1.2 ± 0.03	1.19 ± 0.02
Zirconia test A, $n = 16$	1.25 ± 0.01	1.24 ± 0.17
Zirconia test B, $n = 16$	1.19 ± 0.06	1.18 ± 0.04
p^*	NS	NS
	0.963	0.974

Mean ± standard deviation, *t*-test. No significant differences were found between immediately loaded and unloaded implants.
*$p > .05$.

two planes of different levels, as well zirconia and bone fragments fracture due to differences in hardness between materials. For this reason, the slice thickness for resin-embedded zirconia bone samples in most published papers are in the range of 60–80 µm,[44] 80 µm,[45] 120 ± 20 µm.[46] It may be that this slice thickness affects the bone-implant evaluation at higher levels of detail however for evaluation at lower magnifications as demonstrated in previous works is very useful and commonly applied.

Total peri-implant ST dimensions were evaluated without discriminating between measurements corresponding to connective tissue, epithelial adherence, or sulcus depth in order to evaluate the total thickness, and so adequacy, of the ST mass in direct contact with the implant.

ST thickness evaluation did not reveal differences between implant groups. There was a total thickness corresponding to a biologic width ranging between 2.7 and 3.4 mm, regardless of the surface treatment or whether the implant was of titanium or zirconia.

Immediate loading did not negatively affect ST width, which might be explained by other factors unrelated to loading, such as CBL reduction, plaque accumulation, infection, or inflammation.

Kohal and colleagues[30] analyzed total ST in a 9-month study of monkeys, finding that at the end of the study, the ST collar was of 5 mm thickness for titanium implants and 4.5 mm for zirconia implants of similar dimensions. In the present study, ST dimensions were slightly less due to the animal model used; monkeys have a greater ST thickness in the upper anterior region and the implant design studied had a polished collar that was 3 mm longer than the implants used in the Kohal and colleagues' study.

Total ST was also evaluated in a human study carried out by Bianchi and colleagues,[47] who compared titanium implants with titanium implants with a zirconia collar by means of probe depth and radiography at 0,

TABLE 5 Bone Densities (BD_1) and (BD_2) Related to Loading, Expressed as Percentages

BD Groups	Load	BD_1 %	BD_2 %
Titanium control, $n = 16$	Immediately loaded	63.35 ± 9.38*	58.17 ± 11.5
	Unloaded	59.87 ± 10.66	57.71 ± 13.18
Zirconia test A, $n = 16$	Immediately loaded	59.52 ± 7.82*	57.21 ± 8.74
	Unloaded	56.32 ± 8.13	56.31 ± 7.16
Zirconia test B, $n = 16$	Immediately loaded	73.46 ± 10.3*	59.54 ± 8.92
	Unloaded	69.47 ± 11.25	61.68 ± 10.79

Mean ± standard deviation. Significant differences were obtained. BD_1 with immediate loading was higher compared with BD_2 for all groups without loading. Test B implants showed higher values BD_1 compared with all other groupsBD_2 was similar for all groups without significant differences between groups.
*$p < .05$.

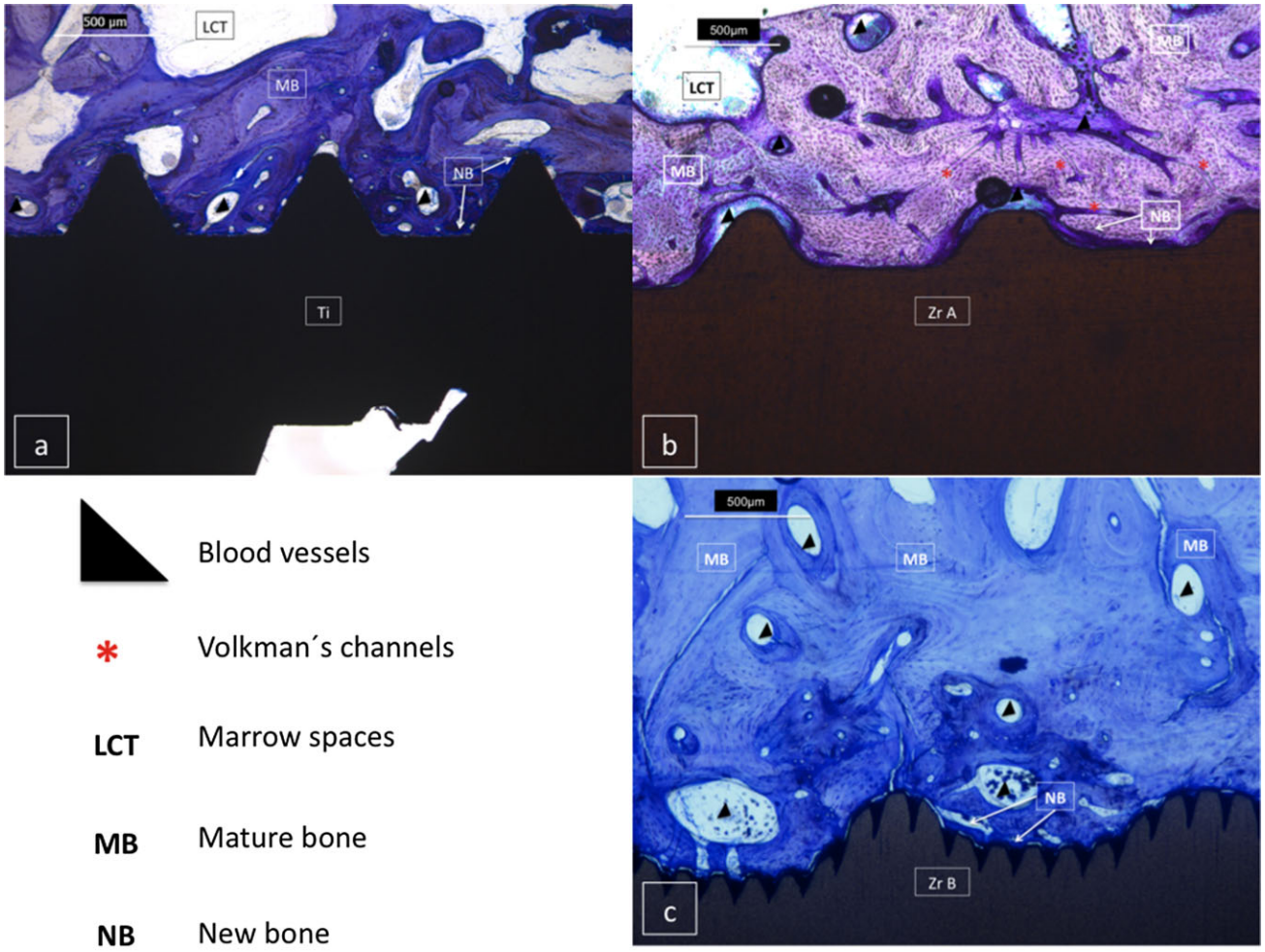

Figure 7 Bone-to-implant contact comparison. All the implants showed direct bone formation on implant surfaces. *A*, Titanium control implants. *B*, Test A with numerous Haversian systems and Volkman's channels in direct contact with implant surface. *C*, Test B with higher bone remodeling and numerous cement lines adjacent to microgrooves. Black triangles indicate blood vessels and lacunae, red dots indicate Volkman's channels. LCT, marrow spaces or lost connective tissue; MB, mature bone; NB, new bone. Toluidine blue stain; ×20 magnification.

6, 12, and 24 months. Probe depth values increased gradually during the first 12 months, and at 24 months, values had established themselves at 2.5 mm for zirconia collar implants and 3.3 mm for titanium implants. The authors attributed this difference to the fact that the zirconia collar implant stabilized the soft issues more effectively thanks to better fibroblast adherence and low bacterial adherence.

In the present study, values for titanium and zirconia implants were similar after 3 months, representing the standard biologic width can be expected in healthy conditions and an absence of inflammation.

Another recent study of two-piece zirconia implants published by Nevins and colleagues[23] found adequate ST union without gingival recession, evaluated by means of probing and radiography. BIC was observed above the implant/abutment junction due to the use of platform switching. BIC was sufficient to produce implant stability but contact was not as strong as the authors had hoped. Unfortunately, although this study is very interesting, it did not include the measurements or evaluations necessary for comparison.

There have been few studies of crestal bone height for zirconia implants inserted in dogs. In the present study, histomorphometric analysis evaluated crestal bone height by measuring the distance from the implant shoulder in the case of zirconia implants, or from the platform in the case of titanium implants, to the first point of BIC in millimeters, and it was found that the addition of microgrooves of 30 mm width did not result in either increased bone loss or in better preservation of crestal bone height.

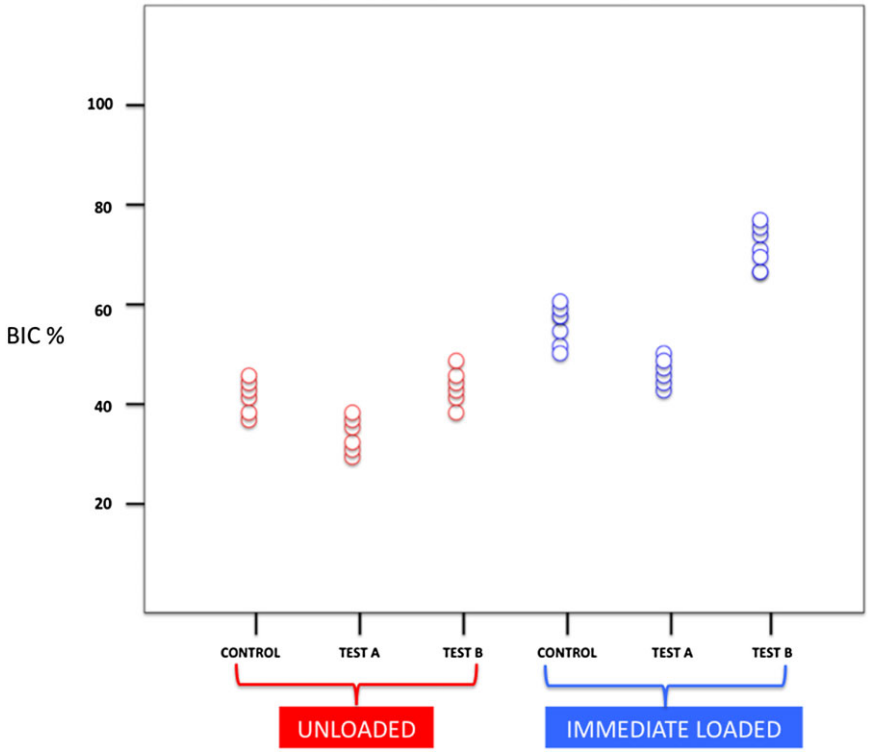

Figure 8 Bone-to-implant contact. Unloaded versus immediately loaded implants. The graph shows the mean values obtained expressed as percentages. Values are higher for immediately loaded test B implants. Toluidine blue stain; ×20 magnification.

Crestal bone heights around zirconia implants inserted in dogs were evaluated in a study carried out by Koch and colleagues,[27] which compared osseointegration of zirconia implants with other zirconia implants with sandblasted surfaces, implants with a surface covering of calcium-releasing titanium oxide and synthetic implants and with one-piece titanium implants. The authors made a distinction between bone loss related to the bone itself and bone loss related with the implant surface treatment. It was found that submerged

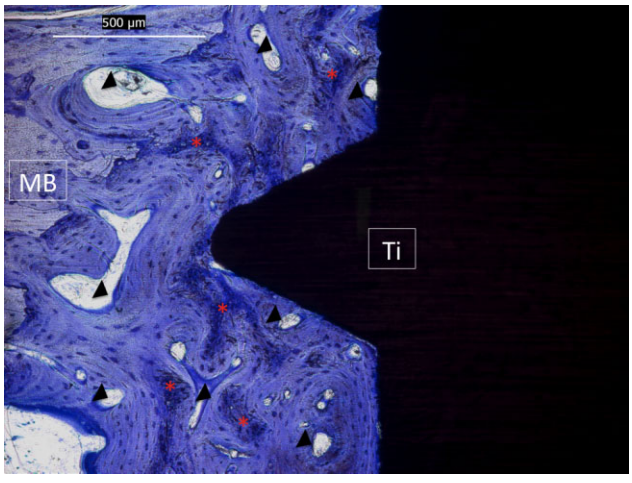

Figure 9 Control thread at high magnification. Black triangles indicate blood vessels and lacunae, red dots indicate vascular growth nodules and tight bone contact with some vessels in direct contact with implant surface. Toluidine blue stain; ×40 magnification.

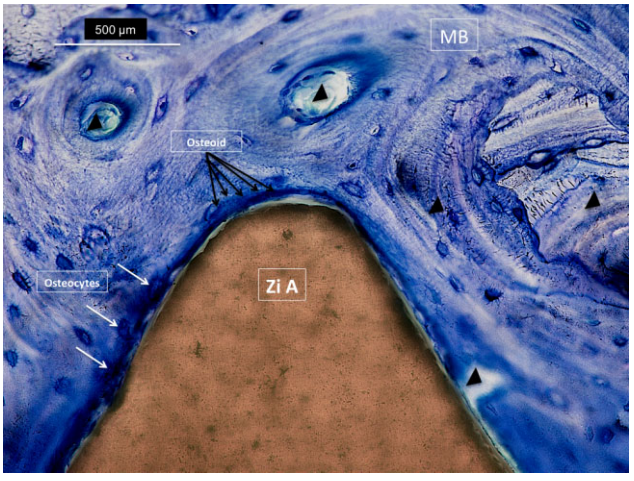

Figure 10 Test A thread at high magnification. Black triangles indicate blood vessels and lacunae, osteoblast bodies appear inside some lacunae; white arrows indicate osteocytes in direct contact with implant surface; osteocytes have aflattened pattern in mature bone; black arrows indicate osteoid deposition with a dark blue color. ×40 magnification.

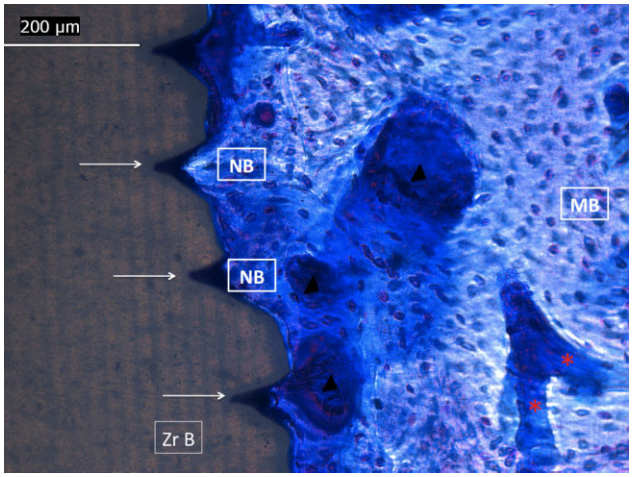

Figure 11 Test B thread at high magnification. Black triangles indicate blood vessels and lacunae, osteoblast bodies appear inside some lacunae; white arrows indicate bony ingrowth inside microgrooves and nested cells inside the microgrooves; red dots indicate vascular and channel formations. ×40 magnification.

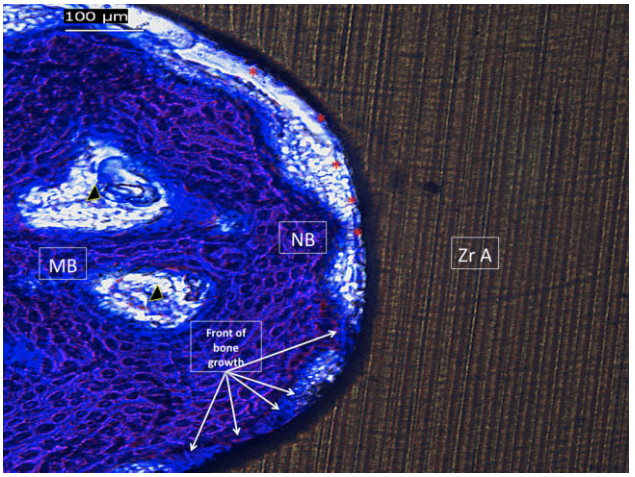

Figure 13 Test A inter-thread zone. Black triangles indicate blood vessels, red dots indicate matrix deposition on implant surface, dark blue color indicates new bone and violet color mature bone. The new bone extends from host bone to implant surface.

implants showed higher bone levels due to the deeper insertion level, with values that varied between 1.3 (synthetic), 0.59 (zirconia with covering), 0.53 (zirconia without covering), and 0.37 mm (titanium). For non-submerged implants the values were 0.37 (titanium), 0 (zirconia with covering), 0.58 (synthetic), 0.59 (titanium), and 0.76 mm (zirconia without covering).

The CBL obtained in the present work agree with previous data. Our results showed similar values for all groups, as all implants were inserted at crestal level these results are probably related to the natural resorptive process that fell within in a specific range of 1.2 ± 0.05 mm for all groups.

Given the neck configuration of one-piece zirconia implants without microgap presence, and the two-piece configuration of titanium implants with a microgap at the implant/abutment junction, might be expected for the titanium implants a different behavior of the CBL which could predispose the CBL. Interestingly, were not observed differences in CBL related to the presence or absence of microgap. Probably because did not were performed abutment

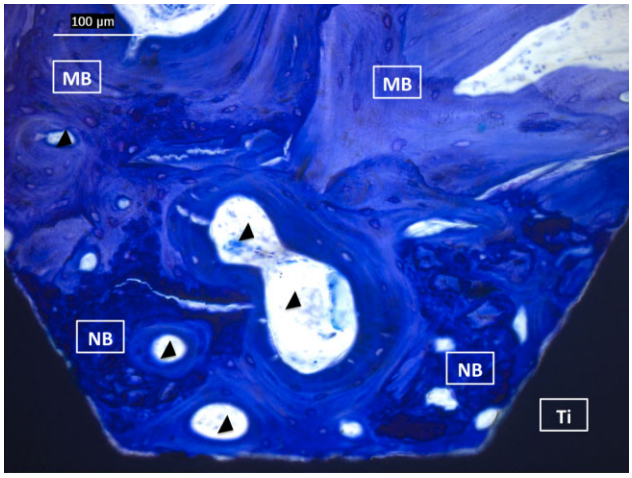

Figure 12 Control inter-thread zone. Black triangles shows blood vessels, dark blue color shows new bone, and cement lines shows lamelar bone growth, light blue shows mature bone with flattened osteocytes.

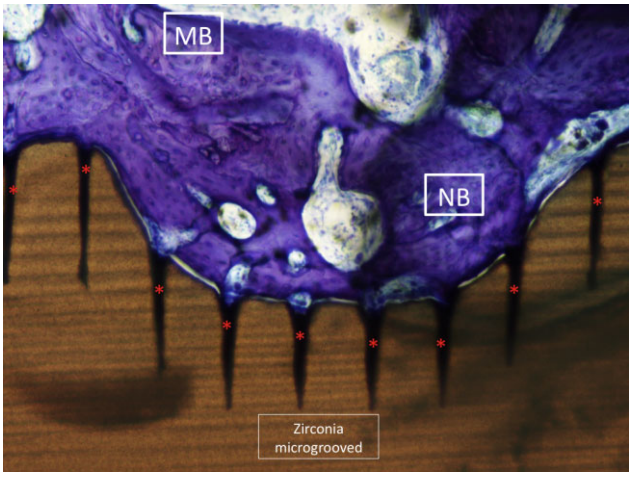

Figure 14 Test B inter-thread zone. Red dots indicate bone growth inside the microgrooves, starting with matrix deposition, cell migration from the host bone, and blood vessels in contact with the implant surface. NB, new bone; MB, mature bone.

disconnections and strict plaque controls were established. These results agree with those obtained by Heijdenrijk and colleagues,[48] who tested the influence of the microgap of two-piece implants placed in a non-submerged approach, in comparison with submerged implants and one-piece implants after a 5-year evaluation of gingival, plaque, and radiographic scores, and concluded that "the microgap at the crestal level in two-piece implants does not appear to have an adverse effect on the amount of peri-implant bone loss during a 5-year period."

BIC for zirconia implants has been evaluated using various animal models. Akagawa and colleagues[49] made a study of implants inserted in monkeys using one-piece zirconia implants splinted to adjoining teeth, evaluating bone contact ratio (BCR), defined as the percentage of BIC along the whole length of the implant, after 12 and 24 months following insertion. They found lower BCR values for mesial-distal BCR 54 ± 10.1% than buccolingual BCR 70.5 ± 7.1%.

In the present study, implants were only splinted to other implants; the results showed higher BIC values than Akagawa's study, probably due to the different surfaces, the animal model and the different study periods, which make comparison difficult.

A study by Koch and colleagues,[27] using dogs, found that 59.24% (mean 59.11 ± 7.45%) of the zirconia implant surfaces presented tight BIC after 6 weeks. A median BIC rate of 58.34% (mean 55.83 ± 13.92%) was measured for calcium-liberating TiO2-coated zirconia implants, a median BIC of 26.82% (mean 26 ± 8.9%) for synthetic implants, and finally, a median BIC of 41.22% (mean 40.91 ± 10.11%) was found with titanium implants. Significant differences were not found between the groups studied, and it was concluded that zirconia implants osseointegrate in the same way as the other groups analyzed.

Comparing this study with the present one, the presence of microgrooves on the zirconia implant surfaces was seen to favor BIC. However, different geometries, animal model and study periods together with differing BIC parameters between the studies make comparison of the two sets of results uncertain.

A study of BIC in zirconia implants inserted in minipig mandible[50] found that BIC values varied according to implant type and whether implants were submerged or not. At 4 weeks following placement, BIC was slightly higher with titanium implants (53%), followed by submerged zirconia implants (52.63%), and the lowest values were found with non-submerged zirconia implants (48%).

However, it is not possible to compare the present study with the minipig study because of the differences in osseous regeneration periods for the animal models studied, which have a relation of 1:3 (pig : dog)[51] as well as the differences in the remodeling process in pigs, osseous remodeling in humans being 1.0–1.5 mm/day, while in pigs it is 1.2–1.5 mm/day and 1.5–2.0 mm/day in dogs.[52]

Gottlow and colleagues[53] studied the biomechanics and osseointegration of a titanium alloy implant containing 13% titanium and 13% zirconia with a diameter of 4.8 mm and length of 6 mm, comparing these with a titanium implant. Both implant types had the same sandblasted and acid-etched hydrophilic surfaces and were inserted in minipigs. The osseous chambers that formed between the implants' spiral threads were analyzed, and at 4 weeks, the authors found BIC values that were statistically higher for titanium/zirconia alloy implants (45.5 ± 13.2%) than titanium implants (40.2 ± 15.2%).

The present study found higher BIC values for test B compared with titanium control and test A implants. These differences could be attributable to the microgrooved surfaces that increased the BIC values for the zirconia implants in test B by guiding and additional bone growth. The 30 mm width of the microgrooves could provide a reduced "jump distance" for osteoblast adherence and migration and a subsequent focus for matrix deposition.

In the present study, BD analysis compared BD_1 (bone adjacent to the implant) and BD_2 (peripheral bone) in two precisely demarcated areas of the same size, which provided additional information about the effects and characteristics of the surface bone immediately adjoining the implant, comparing it with peripheral native bone.

BD adjacent to the implant was seen to increase over the study period in all groups. Differences in implant surface may have affected the transmission of forces, osseous remodeling and subsequent mineralization, the addition of microgrooves and increased surface roughness in the zirconia implants, and the presence of microgrooves and greater surface roughness in titanium implants being positive factors favoring the increase of BD adjacent to implants. Peripheral BD did not vary

over the time span studied and maintained an average of $58 \pm 8\%$ for all groups, which might mean that the effect of the surface modifications extend to a maximum distance of 1.8 ± 0.3 mm into the bone tissue surrounding the implant, which is the distance of the BD_2 area to BD_1 area.

Another factor that may explain differences in BD is variation in implant insertion depth. Gahlert and colleagues[54] compared BD and BIC in titanium and zirconia implants inserted in minipigs at 1, 2, and 3 months following implant placement. Comparing all groups, it was found that if zirconia implants were submerged, they presented a BD of 80% (and submerged titanium 74%), while non-submerged zirconia implants showed a lower value of 63%. In the present study, all implants were inserted at the same level, therefore the variations in BD are more likely to be related to implant surface and immediate loading than implant insertion depth.

Schliepake and colleagues[55] compared peri-implant bone after 4 and 13 weeks with three types of implant: sandblasted zirconia, sandblasted and acid-etched zirconia, and titanium implants, all inserted in minipig mandibles. BD findings varied from $72 \pm 21.6\%$ for sandblasted and acid-etched zirconia, $61.3 \pm 12.4\%$ for sandblasted zirconia implants, to $65.3 \pm 11.3\%$ for the titanium implants. The authors attributed these differences to variations in surface roughness.

This coincides with the present results, whereby at 3 months, test B zirconia implants showed the highest BD values, followed by the control titanium implants and test A zirconia implants. Greater surface roughness was seen to increase BD values in a proportional relation.

The effects of immediate loading on BD in the study showed that for splinted implants of different materials and surfaces, BD increased when subjected to mechanical loading and the implant microgrooved surfaces had an additional effect on BD increase.

Nevertheless, further research is necessary with longer follow-up times to test whether the effects of microgrooves on zirconia implants are lasting and whether or not the presence of microgrooves affects ST, bone remodeling, and BIC integrity in the long term.

Although the results of this work have demonstrated the benefits of microgrooves in zirconia implants, some related problems with color, mechanical strength, and long-term behavior of zirconia implants under mechanical load must be taken in account.

One drawback is whether or not the surface treatment applied can affect the integrity and mechanical properties of the zirconia implant. Zinelis and colleagues[56] made a study of phase transformation, observing commercially manufactured zirconia implants' crystalline phase by means of x-ray diffraction, finding that the intraosseous area treated with sandblasting showed a predominance of tetragonal phase with traces of monoclinic phase, while the implants' machined surface showed tetragonal phase alone; the authors concluded that surface treatment may induce a crystalline phase-change.

However, the zirconia implants used in the present study, femtosecond laser-treated, showed a predominance of tetragonal phase (determined by x-ray diffraction) in the intraosseous portion, which had been previously sandblasted. This may have been due to the elimination of surface areas where monoclinic phase was present, previously modified by sandblasting, to expose underlying layers with a predominance of tetragonal phase.[41]

Although phase transformation affects zirconia's mechanical properties, we have not studied the resistance to fracture of zirconia implants' treated with laser microgrooves – a matter for future research.

The second drawback is the long-term behavior of zirconia implants. It is a known fact that zirconia implants will display an increasing brittleness in bone in situ, the longer time it is inserted. Furthermore, various surface modifications will further increase this brittleness. In the case of aluminum oxide implants used previously, they showed excellent short-term results, but fractured after longer times in situ due to these problems. Whether the same will occur with zirconia is unknown. The short term used in this animal study and the protected occlusion resulted in splinted implants did not provide information on the mechanical behavior of microgrooved zirconia implants.

The third drawback is the gray color over the entire treated area. Elemental analysis of untreated zirconia implants compared with laser-treated implants showed an increase in oxygen levels and a decrease in carbon, which might indicate that the gray color arises from an area of oxidization resulting from laser treatment.[41] This gray color could be eliminated with a heat treatment that reaches 300°C; however, we did not, to assess the biological effects of laser treatment without any modification.

Despite the positive results achieved, zirconia implants should be evaluated with caution until data regarding the clinical long-term behavior are available. However, the study of new surface treatments that do not affect the crystalline phase and mechanical properties are necessary for zirconia dental implants.

CONCLUSIONS

Within the limitations of this study, it may be concluded:

- For all used implants, the ST thickness has a mean of 3 mm related to the establishment of the biologic width.
- A slight CBL reduction will be expected for all implant groups, and the presence of microgrooves in the neck area of zirconia dental implants does not prevent crestal bone remodeling.
- Increased BIC and BD percentages will be expected around all splinted implants with immediate loading at 3 months after implant insertion.
- The addition of microgrooves in the intraosseous portion of sandblasted zirconia dental implants increases the BIC and BD in comparison with sandblasted and acid-etched titanium implants and sandblasted zirconia dental implants.

REFERENCES

1. Albrektsson T, Sennerby L, Wennerberg A. State of the art of oral implants. Periodontol 2000 2008; 47:15–26.
2. Dierens M, Vandeweghe S, Kisch J, Nilner K, De Bruyn H. Long-term follow-up of turned single implants placed in periodontally healthy patients after 16-22 years: radiographic and peri-implant outcome. Clin Oral Implants Res 2012; 23:197–204. doi: 10.1111/j.1600-0501.2011.02212.x
3. Malo P, de Araujo NM, Lopes A, Moss SM, Molina GJ. A longitudinal study of the survival of All-on-4 implants in the mandible with up to 10 years of follow-up. J Am Dent Assoc 2011; 142:310–320.
4. Jacobs R, Pittayapat P, van Steenberghe D, et al. A split-mouth comparative study up to 16 years of two screw-shaped titanium implant systems. J Clin Periodontol 2010; 37:1119–1127.
5. Javed F, Al-Hezaimi K, Almas K, Romanos GE. Is titanium sensitivity associated with allergic reactions in patients with dental implants? A systematic review. Clin Implant Dent Relat Res 2011; 17:1–6.
6. Siddiqi A, Payne AGT, De Silva RK, Duncan WJ. Titanium allergy: could it affect dental implant integration? Clin Oral Implants Res 2011; 22:673–680.
7. Sicilia A, Custa S, Coma G, et al. Titanium allergy in dental implant patients: a clinical study on 1500 consecutive patients. Clin Oral Implants Res 2008; 19:823–835.
8. Flatebo RS, Johannessen AC, Gronningsaeter AG, et al. Host response to titanium dental implant placement evaluated in a human oral model. J Periodontol 2006; 77:1201–1210.
9. Kan JY, Runcharangssaeng K, Lozada JL, Zimmerman G. Facial gingival tissue stability following immediate placement and provisionalization of maxillary anterior single implants: a 2- to 8-year follow-up. Int J Oral Maxillofac Implants 2011; 26:179–187.
10. Nisapakultorn K, Suphanantachat S, Silkosessak O, Rattanamongkolgul S. Factors affecting soft tissue level around anterior maxillary single-tooth implants. Clin Oral Implants Res 2010; 21:662–670.
11. De Rouck T, Eghbali R, Collys K, De Bruyn H, Cosyn J. The gingival biotype revisited: transparency of the periodontal probe through the gingival margin as a method to discriminate thin from thick gingiva. J Clin Periodontol 2009; 36: 428–433.
12. Verdugo F, Simonian K, Nowzari H. Periodontal biotype influence on the volume maintenance of onlay grafts. J Periodontol 2009; 80:816–823.
13. Sailer I, Zembic A, Jung RE, Hämmerle CH, Mattiola A. Single-tooth implant reconstructions: esthetic factors influencing the decision between titanium and zirconia abutments in anterior regions. Eur J Esthet Dent 2007; 2:293–310.
14. Kan JY, Rungcharassaeng K, Umezu K, Kois JC. Dimensions of peri-implant mucosa: an evaluation of maxillary anterior single implants in humans. J Periodontol 2003; 74:557–562.
15. Gittens RA, Olivares-Navarrete R, Tannenbaum R, Boyan BD, Schwartz Z. Electrical implications of corrosion forosseointegration of titanium implants. J Dent Res 2011; 90:1389–1397. doi: 10.1177/0022034511408428
16. Messer RL, Tackas G, Mickalonis J, Brown Y, Lewis JB, Wataha JC. Corrosion of machined titanium dental implants under inflammatory conditions. J Biomed Mater Res B Appl Biomater 2009; 88:474–481.
17. Özkurt Z, Kazazoglu E. Zirconia dental implants: a literature review. J Oral Implantol 2011; 37:367–376.
18. Koutayas SO, Vagkopoulou T, Pelekanos S, Koidis P, Strub JR. Zirconia in dentistry: part 2. Evidence-based clinical breakthrough. Eur J Esthet Dent 2009; 4:348–380.
19. Adatia ND, Bayne SC, Cooper LF, Thompson JY. Fracture resistance of yttria-stabilized zirconia dental implant abutments. J Prosthodont 2009; 18:17–22.
20. van Brakel R, Noordmans HJ, Frenken J, de Roode R, de Wit GC, Cune MS. The effect of zirconia and titanium implant abutments on light reflection of the supporting soft tissues. Clin Oral Implants Res 2011; 22:1172–1178. doi: 10.1111/j.1600-0501.2010.02082

21. Manicone PF, Rossi Iommetti P, Rafaelli L, et al. Biological considerations on the use of zirconia for dental devices. Int J Immunopathol Pharmacol 2007; 20:9–12.
22. Kohal RJ, Baechle M, Han JS, Hueren D, Huebner U, Butsz F. In vitro reaction of human osteoblasts on alumina-toughened zirconia. Clin Oral Implants Res 2009; 20:1265–1271.
23. Nevins M, Camelo M, Nevins ML, Schupbach P, Kim DM. Pilot clinical and histological evaluations of a two-piece zirconia implant. Int J Periodontics Restorative Dent 2011; 31:157–163.
24. Oliva J, Oliva X, Oliva JD. Five-year success rate of 831 consecutively placed zirconia dental implants in humans: a comparison of three different rough surfaces. Int J Oral Maxillofac Implants 2010; 25:336–344.
25. Salihoglu U, Boynuegri D, Engin D, Duman AN, Gokalp P, Balos K. Bacterial adhesion and colonization differences between zirconium oxide and titanium alloys: an in vivo human study. Int J Oral Maxillofac Implants 2011; 26:101–107.
26. Scarano A, Piatelli M, Caputi S, Favero GA, Piatelli A. Bacterial adhesion on commercially pure titanium and zirconium disks: an in vivo human study. J Periodontol 2004; 75:292–296.
27. Koch FP, Weng D, Krämer S, Biesterfeld S, Jahn-Eimermacher A, Wagner W. Osseointegration of one-piece zirconia implants compared with a titanium implant of identical design: a histomorphometric study in the dog. Clin Oral Implants Res 2010; 21:350–356.
28. Hoffmann O, Angelov N, Gallez F, Jung RE, Weber FE. The zirconia implant-bone interface: a preliminary histological evaluation in rabbits. Int J Oral Maxillofac Implants 2008; 24:691–695.
29. Minamizato T. Slip-cast zirconia dental roots with tunnels drilled by laser process. J Prosthet Dent 1990; 63:677–684.
30. Kohal RJ, Weng D, Bächle M, Strub JR. Loaded custom-made zirconia and titanium implants show similar osteointegration: an animal experiment. J Periodontol 2004; 75:1262–1268.
31. Sennerby L, Dasmah A, Larsson B, Iverhed M. Bone tissue responses to surface modified zirconia implants: a histomorphometrical and removal torque study in the rabbit. Clin Implant Dent Relat Res 2005; 7:13–20.
32. Gahlert M, Gudehus T, Eichhorn S, Steinhauser E, Kniha H, Erhardt W. Biomechanical and histomorphometric comparison between zirconia implant with varying surface textures and a titanium implant in the maxilla of minipigs. Clin Oral Implants Res 2007; 18:662–668.
33. Ferguson SJ, Langhoff JD, Voelter K, et al. Biomechanical comparison of different surface modifications for dental implants. Int J Oral Maxillofac Implants 2008; 23:1037–1046.
34. Kohal RJ, Wolkewitz M, Hinze M, Han J-S, Bächle M, Butz F. Biomechanical and histological behavior of zirconia implants. An experiment in the rat. Clin Oral Implants Res 2009; 20:333–339.
35. Lee J, Sieweke JH, Rodriguez NA, et al. Evaluation of nano-technology-modified zirconia oral implants: a study in rabbits. J Clin Periodontol 2009; 36:610–617.
36. Rocchietta I, Fontana F, Addis A, Schupbach P, Simion M. Surface modified zirconia implants: tissue response in rabbits. Clin Oral Implants Res 2009; 20:844–850.
37. Pirker W, Wiedemann D, Lidauer A, Kocher AA. Immediate, single stage, truly anatomic zirconia implant in lower molar replacement: a case report with 2.5 years follow-up. Int J Oral Maxillofac Surg 2011; 40:212–216.
38. Silva NR, Coelho PG, Fernandes CA, Navarro JM, Dias RA, Thompson VP. Reliability of one-piece ceramic implant. J Biomed Mater Res B Appl Biomater 2009; 88:419–426.
39. Zhu J, Yang DW, Ma F. Feasibility study of a partially hollow configuration for zirconia dental implants. J Oral Maxillofac Surg 2010; 68:399–406.
40. Wenz HJ, Bartsch J, Wolfart S, Kern M. Osseointegration and clinical success of zirconia dental implants. Int J Prosthodont 2008; 21:27–36.
41. Delgado-Ruíz RA, Calvo-Guirado JL, Moreno P, et al. Femtosecond laser microstructuring of zirconia dental implants. J Biomed Mater Res B Appl Biomater 2011; 96:91–100.
42. Valderrama P, Bornstein M, Jones AA, Wilson TG, Higginbottom FL, Cochran DL. Effects of implant design on marginal bone changes around early loaded, chemically modified, sandblasted acid-etched-surfaced implants: a histologic analysis in dogs. J Periodontol 2011; 82:1025–1034.
43. Nelson K, Semper W, Hildebrand D, Ozyuvaci H. A retrospective analysis of sand-blasted, acid-etched implants with reduced healing times with an observation period of up to 5 years. J Oral Maxillofac Implants 2008; 23:726–732.
44. Hoffmann O, Angelov N, Zafiropoulos G, Andreana S. Osseointegration of zirconia implants with different surface characteristics: an evaluation in rabbits. Int J Oral Maxillofac Implants 2012; 27:352–358.
45. Saulacic N, Bosshardt D, Bornstein M, Berner S, Buser D. Bone apposition to a titanium-zirconium alloy implant, as compared to two other titanium-containing implants. Eur Cell Mater 2012; 23:273–288.
46. Gahlert M, Roehling S, Sprecher CM, Kniha H, Milz S, Bormann K. In vivo performance of zirconia and titanium implants: a histomophometric study in mini pig maxillae. Clin Oral Implants Res 2012; 23:281–286.
47. Bianchi AE, Bosetti M, Dolci G, Sberna MT, Sanfilippo F, Cannas M. In vitro and in vivo follow-up of titanium transmucosal implants with a zirconia collar. J Appl Biomater Biomech 2004; 2:143–150.
48. Heijdenrijk K, Raghoebar GM, Meijer HJ, Stegenga B, van der Reijden WA. Feasibility and influence of the

microgap of two implants placed in a non-submerged procedure: a five-year follow-up clinical trial. J Periodontol 2006; 77:1051–1060.

49. Akagawa Y, Hosokawa R, Sato Y, Kamayama K. Comparison between freestanding and tooth-connected partially stabilized zirconia implants after two years' function in monkeys: A clinical and histologic study. J Prosthet Dent 1998; 80:551–558.
50. Stadlinger B, Hennig M, Eckelt E, Kunlisch E, Mai R. Comparison of zirconia and titanium implants after a short healing period. A pilot study in minipigs. Int J Oral Maxillofac Surg 2010; 39:585–592.
51. Turner AS. Animal models of osteoporosis. Necessity and limitations. Eur Cells Mater 2001; 1:66–81.
52. Pearce AI, Richards RG, Milz S, Schneider E, Pearce SG. Animal models for implant biomaterial research in bone. Eur Cells Mater 2007; 13:1–10.
53. Gottlow J, Dard M, Kjellson F, Obrecht M, Sennerby L. Evaluation of a new titanium-zirconia implant: a biomechanical and histological comparative study in the minipig. Clin Implant Dent Relat Res 2012; 14:538–545.
54. Gahlert M, Rohling S, Wieland M, Sprecher CM, Kniha H, Milz S. Osseointegration of zirconia and titanium dental implants: a histological and histomorphometrical study in the maxilla of pigs. Clin Oral Implants Res 2009; 20:1247–1253.
55. Schliephake H, Hefti T, Schlottig F, Gédet P, Staedt H. Mechanical anchorage and peri-implant bone formation of surface-modified zirconia in minipigs. J Clin Periodontol 2010; 37:818–828.
56. Zinelis S, Thomas A, Syres K, Silikas N, Eliades G. Surface characterization of zirconia dental implants. Dent Mater 2010; 26:295–305.